

Critical Impeller Speed for Solid Suspension in Mechanically Agitated Contactors

Critical impeller speed for the suspension of solid particles, N_{CS} , has been measured in 0.3, 0.4, 0.57, 1.0, and 1.5 m ID mechanically agitated contactors. Tap water and quartz particles (100, 340, 700, 850, 2,000 μm) were used as liquid and solid phase, respectively. The impeller speed was varied from 3.5 to 13.3 r/s and solid loading from 0 to 50 wt. %. Three types of impellers were employed: disk turbine, pitched turbine downflow, and pitched turbine upflow. The impeller diameter to vessel diameter ratio was varied in the range 0.175 to 0.58 and the impeller blade width to impeller diameter ratio was varied in the range 0.25 to 0.4. The impeller clearance from the tank bottom was varied from 0.5 to 0.167 of tank diameter. The effect of impeller blade thickness was also studied.

The pitched-blade impellers were found to be more efficient than a conventional disk turbine, and the pitched turbine downflow type was found to be more efficient than a pitched turbine upflow impeller. An attempt has been made to explain the mechanism of suspension on a rational basis and a correlation has been proposed for the estimation of N_{CS} that is expected to be useful in design.

**K. S. M. S. Raghava Rao,
V. B. Rewatkar, J. B. Joshi**

Department of Chemical Technology
University of Bombay
Bombay, India 400 019

Introduction

Mechanically agitated solid-liquid contactors are widely used in industry. The solid phase may be a catalyst or may be material undergoing physical or chemical process. Some examples of such systems in the chemical process and related industries include coal-water slurries, suspension of ion-exchange resins, paper-pulp slurries, polymer dispersions, sugar crystal slurries, and others. Various ore-processing industries also employ such contactors. In all these cases, it is required that the solid particles be completely suspended.

Although solid suspension has been extensively studied in the past for the solid-liquid system, relatively less information is available on the performance of axial-flow turbines, which are known to be efficient for solid suspension. In the past, the solid suspension has been studied using conventional impellers such as the disk turbine, the propeller, etc., and pitched-blade turbines have received scant attention. Therefore, it was thought desirable to study systematically the critical impeller speed for solid suspension, N_{CS} , using pitched-blade turbines. An investi-

gation of the disk turbine was also made for the purpose of comparison.

Depending on the application—such as promoting a chemical reaction between the phases, promoting dissolution or crystal growth, or obtaining a uniform particle concentration in an effluent stream—the suspension can be distinguished as either complete off-bottom suspension or relatively uniform suspension. In the present work, the former was taken as the suspension criterion in determining the critical impeller speed N_{CS} ; it was first used by Zwietering (1958). It has been observed (Kneule, 1956; Harriott, 1962) that below the critical impeller speed, the total surface area of solids is not available for processing. However, above this speed the rate of mass transfer processes increases very slowly. Therefore, any additional energy beyond that required for N_{CS} is not useful and consequently knowledge of N_{CS} is very important.

In the past, most of empirical correlations for N_{CS} have been developed using small-scale equipment and there has been a paucity of data to confirm the correlations on large-scale contactors. Therefore, the present investigation is concerned with experimentation on a large scale and with understanding the effect of scale. In addition, the mechanism of suspension has been explained on a rational basis. An attempt has been made to

Correspondence concerning this paper should be addressed to J. B. Joshi.

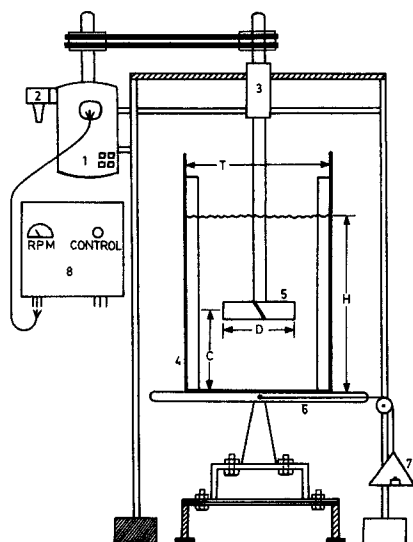


Figure 1. Experimental set-up

- | | |
|----------------------|--------------------|
| 1. D.C. motor | 5. Impeller |
| 2. Motor cooling fan | 6. Torque table |
| 3. Bearing support | 7. Weights and pan |
| 4. Tank | 8. Thyristor panel |

understand the effects of various parameters such as average particle size d_p , impeller diameter D , tank diameter T , and solids loading X , on N_{CS} , the critical impeller speed for solids suspension. Correlations have been proposed for N_{CS} that are expected to be useful for design.

Experimental Set-up and Procedure

The experimental set-up is shown in Figure 1. Experiments were carried out in 0.3, 0.4, 0.57, 1.0, and 1.5 m ID mechanically agitated contactors (MAC) fitted with four baffles of standard width. Three types of impellers were employed: disk turbine (DT), pitched-blade turbine, downflow (PTD), and

Table 1. Design Details of Mechanically Agitated Contactors

Diameters, m	0.3, 0.4, 0.57, 1.0, 1.5
H/T	1
Baffle width, % tank dia	10
No. baffles	4
Material	Transparent acrylic
Geometry	Cylindrical with flat bottom
Impeller position, from tank bottom	$T/6, T/4, T/3, T/2$

pitched-blade turbine, upflow (PTU). Details pertaining to the design of MAC and impellers are given in Tables 1 and 2, respectively. The impeller speed and solids loading were varied in the range 3.5 to 13.3 r/s and 0–50 wt. %, respectively. Tap water and quartz particles were used as the liquid and solid phases. Details pertaining to the solids particles are shown in Table 3.

The critical impeller speed for solids suspension, N_{CS} , was defined as the speed at which no solids remained stationary on the base of MAC for longer than 2 s (Zwietering, 1958). Measurements of N_{CS} were made by visually observing the solids suspension by placing a mirror below the tank base, which was well illuminated.

At a constant loading of solids particles, when the impeller speed is gradually increased, more and more particles are suspended. The position of the suspension of the last particles depends on the impeller design. In case of DT and PTU impellers, the particles are suspended from an annular space around the center of the tank bottom, whereas for a PTD impeller suspension occurs from the periphery of the tank bottom. As the speed increases the amount of solids present on the tank bottom gradually reduces. When a particular impeller speed is reached, all the particles move vigorously on the tank bottom before being suspended. However, during their path they momentarily stop for a while (which is prominent enough to be noticed) before becoming suspended. With a slight increase in the impeller speed, this momentary stoppage of solid particles is eliminated.

Table 2. Design Details of Impellers Used

Impeller	No. Blades	Dia., D m	Blade Width, W m	Blade Length, l m	Blade Thickness, k m
Disk turbine (DT)	6	0.1900	$D/5$	$D/4$	2.3×10^{-3} *
		0.285	$D/5$	$D/4$	2.3×10^{-3} *
Pitched turbine, upflow (PTU)	6	0.1900	0.057	0.075	2.3×10^{-3}
Pitched turbine, downflow (PTD)	6	0.100	0.030	0.030	2.3×10^{-3}
		0.142	0.042	0.046	2.3×10^{-3}
		0.190	0.057	0.075	2.3×10^{-3}
		0.250	0.075	0.100	2.3×10^{-3}
		0.330	0.099	0.142	2.3×10^{-3}
		0.375	0.113	0.165	0.0023
		0.500	0.152	0.227	0.0023
		0.190	0.048	0.07	0.0028
		0.190	0.076	-do-	0.0028
		0.190	0.067	-do-	0.0028
		0.190	-do-	-do-	0.0043
		0.190	-do-	-do-	0.0064
		0.330	0.083	0.142	0.0023
		0.330	0.117	0.142	0.0023

*DT disk thickness = 3×10^{-3} m
PTU, PTD angle of pitch = 45°

Table 3. Details of Solids Particles Used

Type	Avg. Particle Size, d_p μm	Terminal Settling Velocity in Water mm/s
Quartz, granular, density $\rho_s = 2,520 \text{ kg/m}^3$	100	34
	340	76
	700	104
	850	134
	2,000	165

The experimental values of N_{CS} for a disk turbine impeller match quite well (within 11%) with those obtained from Zwietering's equation, as shown in Table 4.

The values of N_{CS} were also obtained from power consumption measurements. The power consumption was measured using a frictionless torque table, and the method of obtaining the values of N_{CS} from power consumption measurements is given below.

Power consumption was measured by increasing the impeller speed gradually at constant solids loading. With increasing speed, the value of N_{PSL} , the power number in the solid-liquid system, gradually increases as more and more particles are suspended, and it flattens off when solids suspension is complete. The speed corresponding to this situation gives the value of N_{CS} . A typical graph is shown in Figure 2. The values of the critical impeller speed for solids suspension thus obtained match very well with those obtained by visual observations ($\pm 5\%$).

Previous Work

The suspension of solids particles in a two-phase (solid-liquid) system has been studied extensively in the past. Zwietering (1958), Narayanan et al. (1969), Weismann and Efferding (1960), Kolar (1961), Nienow (1968), Bourne and Sharma (1974), Baldi et al. (1978), Subbarao and Taneja (1979), Bohnet and Niesmak (1980), Einkenel (1980), Chapman et al. (1983), Musil et al. (1984), and Chudacek (1985) all have investigated solids suspension. These studies have been critically reviewed by Joshi et al. (1982) and Gray and Oldshue (1986). It has been shown that the following type of correlation developed by Zwietering (1958) is useful:

$$N_{CS} = \frac{s\gamma^{0.1}d_p^{0.2}(g\Delta\rho/\rho_L)^{0.45}X^{0.13}}{D^{0.85}} \quad (1)$$

The exponents over γ , d_p , ρ , and X have been found to be

Table 4. Comparison of Experimental N_{CS} with Zwietering's Equation

Loading X wt. %	Avg. Particle Size, d_p μm	$N_{CS}(\text{SL})^*$	
		Zwietering's Eq.	Present Work
0.34	100	2.20	2.45
3.40	700	2.95	3.33
0.34	700	3.25	3.61
3.40	2,000	4.35	4.83
0.34	2,000	4.00	4.41

Disk turbine impeller; $T = 0.57 \text{ m}$, $C = T/3$, $D = T/2$

*Solid-liquid system

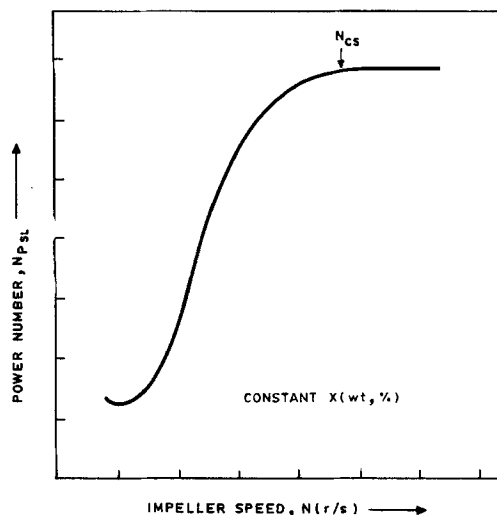


Figure 2. Variation of power consumption with increasing impeller speed at constant solids loading.

practically independent of impeller diameter, vessel size, and impeller clearance. All the variations in the system geometry and impeller design have been included in the parameter s .

Results and Discussion

Effect of impeller design

The comparison of impellers with regard to their suspension ability is shown in Figure 3. The effect of particle size and loading also has been included in the figure. It can be seen that the power required for suspension by a PTD impeller is much lower than required by PTU and DT impellers. For instance, a PTD impeller needs approximately one-fifth as much power for suspending 2,000 μm particles at a loading of 6.6% as does a DT impeller, and one-third as much power compared with a PTU impeller.

The suspension ability of impellers can now be compared on the basis of suspension mechanism. In the case of a disk turbine, the liquid flow generated by the impeller travels in the radial direction and splits into two streams. Each stream creates a cir-

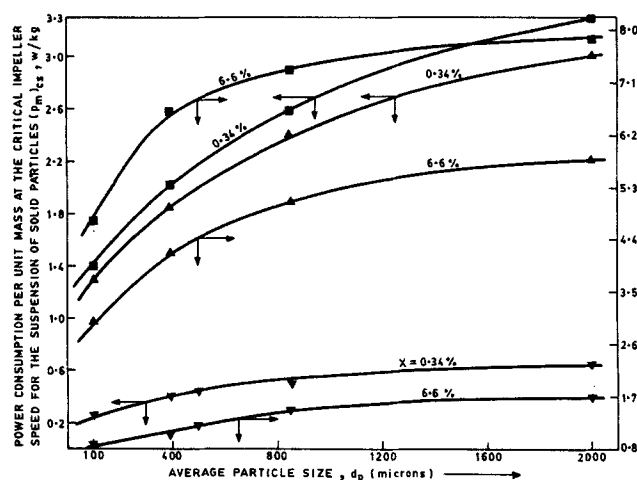


Figure 3. Comparison of impeller suspension abilities.

$T = 0.57 \text{ m}$; $D = T/3$; $C = T/3$

▼ PTD; ▲ PTU; ■ DT

culation loop, one below and one above the impeller. As a result, only a part of the energy supplied by the impeller (which is associated with the lower circulation loop) is available for the suspension. Secondly, the liquid-phase turbulence is generated at the impeller tip and it decays along the path of liquid flow. Further, there is a loss of energy during the two changes in the flow direction, first near the wall opposite impeller and then at the corner of the base and wall. Because of the above three factors the suspension ability of a disk turbine is very poor.

Pitched-blade turbines, both PTU and PTU types at the same power consumption, generate liquid flow and turbulence of comparable magnitude. However, the PTU flow starts from the impeller, travels up (away from the tank base), then changes direction and goes toward the wall. Again it changes direction and flows downward near the wall to the bottom and is now available for the solids suspension. In the case of a PTD impeller the liquid flow is directed toward the tank bottom and is directly available for suspension. The length of the liquid path and the number of direction changes are greater in the case of PTU flow than in PTD flow. In addition, turbulence is generated below the impeller in the case of PTD flow, whereas the turbulence is generated above the impeller in the case of PTU flow. Therefore, a PTD impeller is more efficient for solids suspension than a PTU or DT impeller.

Effect of particle size and loading

The effect of particle size on N_{CS} is shown in Figure 4 for a few typical loadings. With an increase in particle size the settling velocity increases. Therefore, higher average liquid velocity is required to suspend the particles. Thus, N_{CS} values increase with an increase in d_p , the average particle size. Similarly, the effect of solids loading is shown in Figure 5 for a few typical particle sizes. Both these effects of particle size and loading were found to be similar to those reported by Zwietering (1958).

For a given d_p , with an increase in solids loading the liquid flow generated by impeller decreases. This is because some of the impeller energy dissipates at the solid-liquid interface. In order to prove this point liquid-phase mixing time was measured

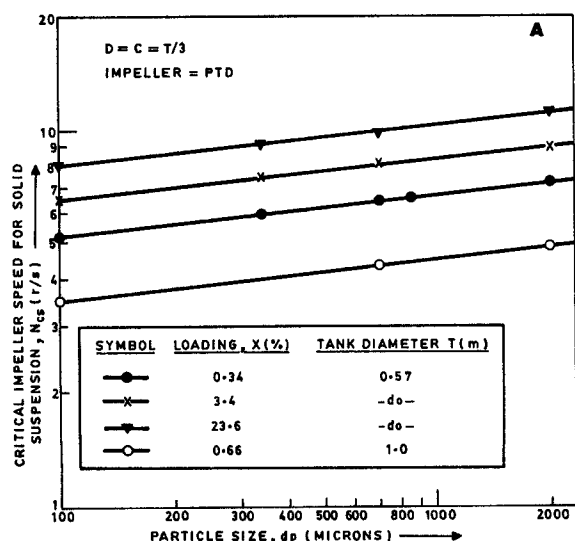


Figure 4a. Effect of particle size on critical impeller speed for solids suspension, PTD impeller.

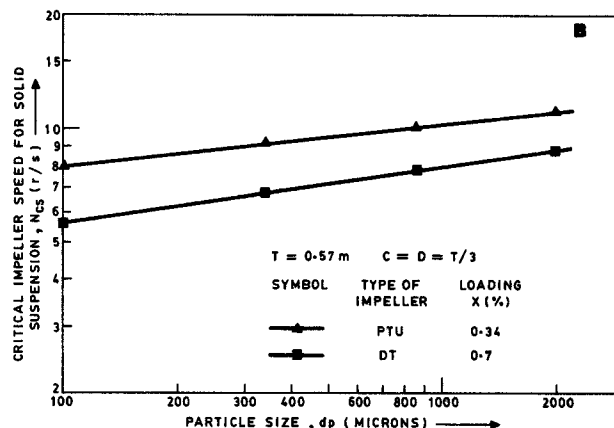


Figure 4b. Effect of particle size on critical impeller speed for solids suspension, PTU, DT impellers.

over a wide range of solids loading and particle size in 0.57 m tall, 1.0 m ID vessels. The details pertaining to the mixing time measurements are reported by Pandit and Joshi (1983). The results are shown in Figure 6 and can be correlated by the following relation:

$$\theta_{mix} \propto X^{0.1} \quad (2)$$

It can be seen that the circulation velocity decreases with an increase in solids loading. Therefore, the critical speed for suspension also increases with increasing solids loading. It may be interesting to note that the dependence of critical impeller speed and liquid-phase mixing time is practically the same.

Effect of impeller clearance

It was observed that the critical impeller speed N_{CS} strongly depends upon the impeller clearance from bottom. The values of the exponents in Eq. 1 do not change appreciably with the location and there is a change only in the proportionality constant. Typical values of N_{CS} have been plotted against the impeller clearance in Figure 7a. It can be seen from this figure that the value of N_{CS} decreases with a decrease in the impeller clearance for all the impellers. However, the extent of reduction is more

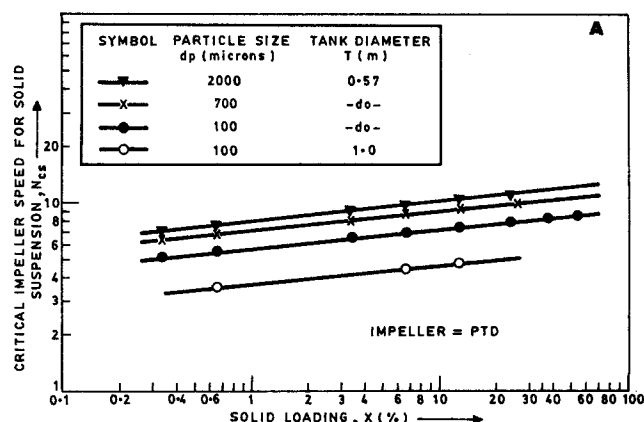


Figure 5a. Effect of solids loading on critical impeller speed for solids suspension, PTD impeller.

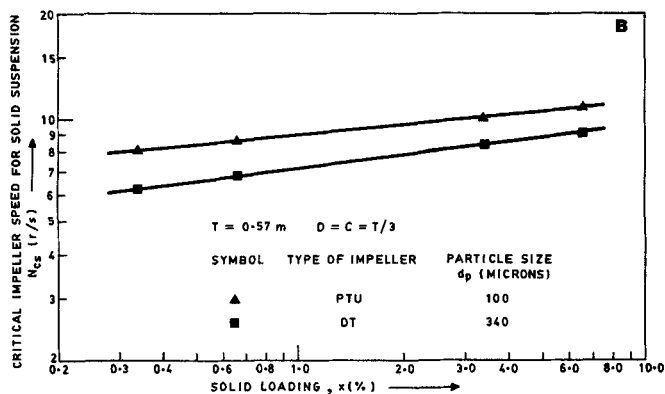


Figure 5b. Effect of solids loading on critical impeller speed for solids suspension, PTU, DT impellers.

for DT and PTU impellers than for a PTD impeller. In the case of a DT, the length of the flow path before it reaches the bottom is $[(T/2) - (D/2) + C]$. With a decrease in clearance the path length decreases. The decrease in loop length causes a dual effect: the decay of turbulence along the flow path (which plays a major role in solids suspension in DT flow) reduces and the liquid velocity increases. The effect of clearance for a DT impeller is further illustrated in the next section.

From the foregoing discussion, it is clear that the flow characteristics are more sensitive to impeller clearance in the case of PTU and DT impeller, whereas, the dependence is less pronounced in the case of a PTD impeller.

Zwietering (1958) has observed a decrease in N_{CS} with a decrease in clearance for propellers and no effect of clearance in the case of a DT. However, Nienow (1968) and Chapman et al. (1983) have observed a decrease in N_{CS} with decreasing clearance for a DT.

The effect of clearance for PTD impellers of different diameter is shown in the Figure 7b for few typical conditions. It can be seen from this figure that the variation of N_{CS} with impeller clearance depends on the impeller diameter at higher clearance ($C = T/2$). The PTD ($T/3$) impeller has the least dependence. However, in the lower range of impeller clearance the dependence of N_{CS} on impeller clearance is almost the same for all PTD impellers (of different diameter).

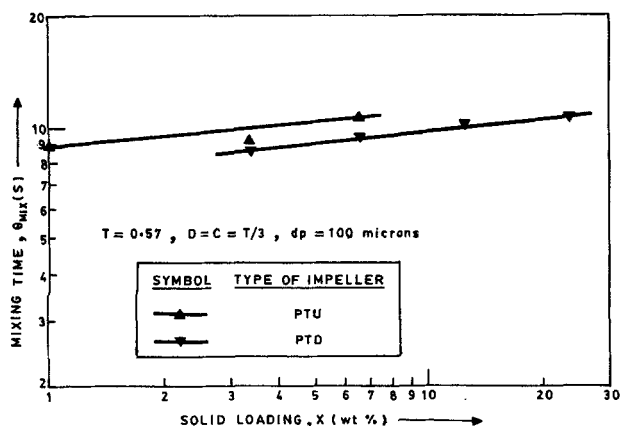


Figure 6. Effect of solids loading on mixing time.

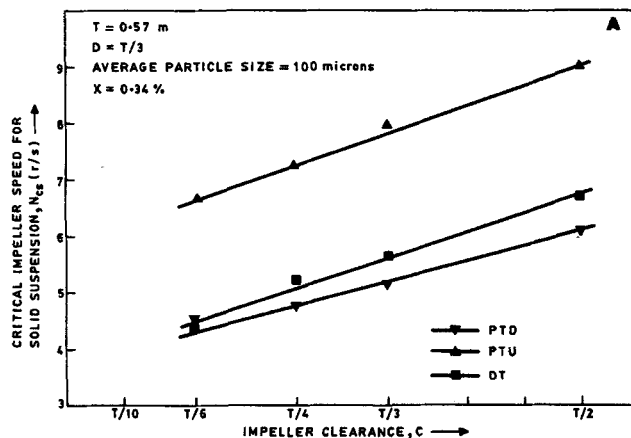


Figure 7a. Effect of impeller clearance from tank bottom on critical impeller speed for solids suspension.

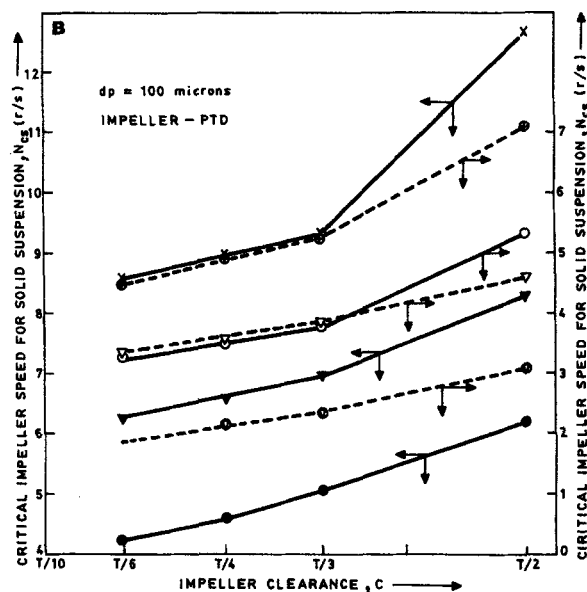


Figure 7b. Effect of PTD impeller clearance from tank bottom on critical impeller speed for solids suspension.

	Impel. Dia., D m	Solids Load., X wt. %	Tank Dia., T m
x	0.1425	6.6	0.57
▼	0.19	6.6	0.57
●	0.25	6.6	0.57
○	0.33	6.6	0.57
▽	0.33	1.3	1.0
⊕	0.25	1.3	1.0
⊗	0.5	1.3	1.0

Kolar (1961) has observed the N_{CS} to decrease with decreasing clearance in case of a PTD impeller (45° , four blades) with little effect of D/T ratio. In the case of propeller a decrease in N_{CS} was found only when $D/T > 0.2$. Moreover, when $D/T < 0.2$ he observed the N_{CS} to increase with a decrease in clearance. The latter observation could be attributed to the suspension criterion that was employed.

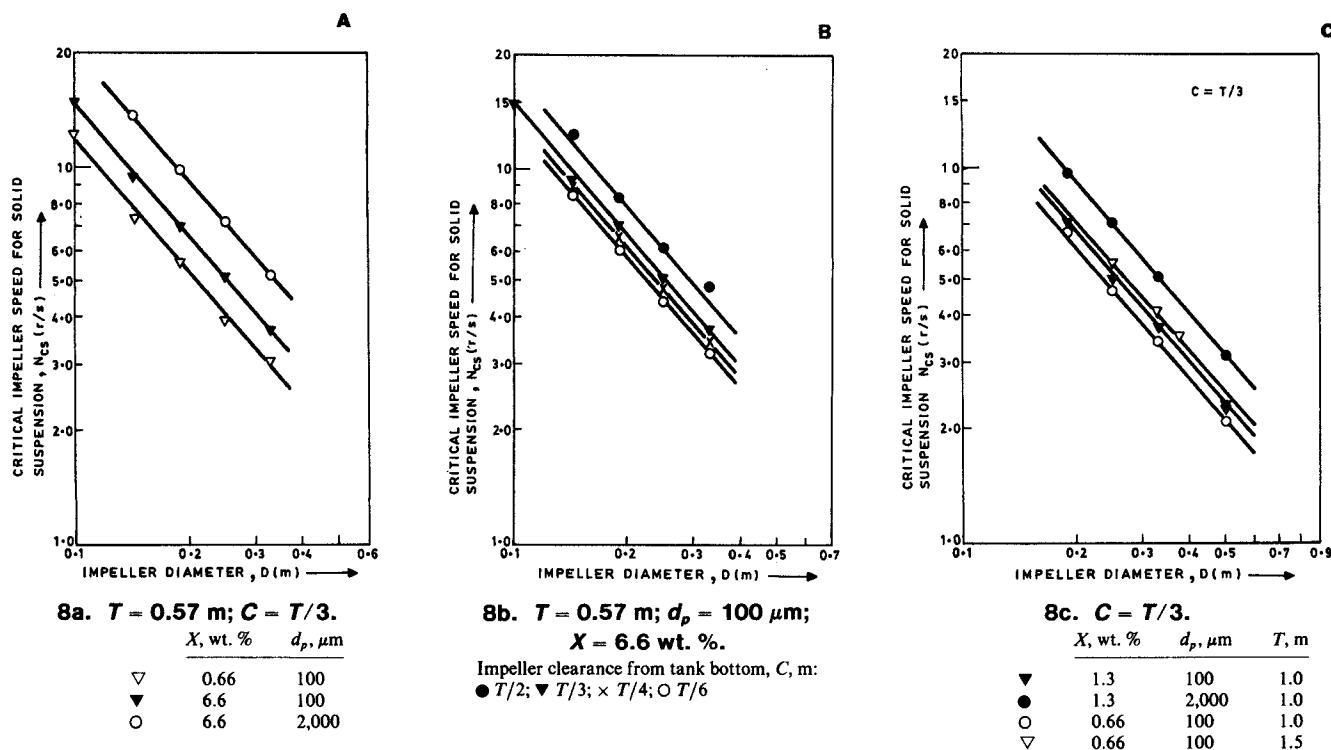


Figure 8. Effect of PTD impeller diameter at constant tank diameter on critical impeller speed for solids suspension.

Effect of impeller diameter

Since PTD flow was found to be more efficient for solids suspension, Figures 3 and 7a, the effects of impeller diameter and vessel diameter were investigated using a PTD impeller. In order to study the effect of impeller diameter, PTD impellers of 0.10, 0.143, 0.19, 0.25, 0.33, 0.375, and 0.5 m dia. were employed in the 0.57, 1.0, and 1.5 m ID vessels. The typical results are shown in Figures 8a, b, c and can be correlated by the following expression:

$$N_{CS} \propto D^{-1.16} \quad (3)$$

It can be seen from Figure 8 that Eq. 3 holds for different particle sizes d_p , loadings X , tank diameters T , and impeller clearances C .

For axial-flow impellers pumping downward (propellers), Zwietering observed the following relationship between the proportionality constant s , Eq. 1, and the vessel to impeller diameter ratio:

$$s \propto (T/D)^{0.82} \quad (4)$$

and his equation gives the following relationship between N_{CS} and D :

$$N_{CS} \propto D^{-0.85} \quad (5a)$$

From Eqs. 3 and 4 we get

$$N_{CS} \propto D^{-1.67} \quad (5b)$$

Recently, Chapman et al. (1983) have reported the exponent

over D to be -1.5 . Thus, the value of the exponent obtained in the present work is lower than those obtained by Zwietering (1958) and Chapman et al. (1983). It may be pointed out that Zwietering used propellers, whereas Chapman et al. used a PTD impeller with four blades. In case of a DT, Zwietering (1958) and Chapman et al. (1983) have obtained exponents over D of -2.35 and -2.45 , respectively.

It will be interesting to understand the effect of impeller diameter on the solid suspension for different designs of impellers. In the case of a disk turbine, the liquid flow is completely radial at the impeller and travels to the wall, where it splits into two streams; one stream goes toward the bottom and one toward the top. The liquid stream going to the bottom is responsible for solids suspension. The length of the flow path before it reaches the bottom is $[(T/2) - (D/2) + C]$.

The solids suspension occurs because of the liquid flow and turbulence. However, the turbulence intensity decays along the length of the flow path. With an increase in the impeller diameter, less decay in the turbulence will occur because of a reduction in path length. Moreover, the liquid velocity also increases with an increase in the impeller diameter ($V_r \propto D^{1/6}$). The overall effect of increased liquid velocity and the lesser decay in turbulence makes the dependence on impeller diameter very strong. It may be pointed out that the change in path length because of a change in impeller diameter will be more and more pronounced with a decrease in clearance $[L = (T/2) - (D/2) + C]$. As a result, the effect of impeller diameter becomes stronger as the clearance is reduced.

In the case of a pitched-blade turbine downflow impeller, the solids suspension occurs mainly because of the liquid flow generated by the impeller. The average liquid velocity is proportional to ND . Therefore, the N_{CS} should be inversely proportional to D . The observed dependence of $D^{-1.16}$ is close to the above reason-

ing. It is obvious that the length of the liquid path will not change appreciably with changes in the PTD impeller diameter, because the liquid flow is downward directly from the impeller. A small change in path may occur because of changes in the blade width (W/D kept constant).

Effect of tank diameter

The effect of tank diameter was studied in two ways. In the first set of experiments D was kept constant. In the second set, D/T was maintained constant. In the first set, a 0.33 m PTD impeller was used in 0.57, 1.0, and 1.5 m dia. tanks with a clearance of $T/3$. The results are shown in Figure 9. The following relationship was obtained:

$$N_{CS} \propto T^{0.31} \quad (6)$$

In the second set, the value of D/T was maintained at $1/3$ and the impeller clearance was $T/3$. The following relationship was obtained, Figure 10:

$$N_{CS} \propto T^{-0.82} \quad (7)$$

The exponent in Eq. 6 is positive whereas that in Eq. 7 is negative. In the first set (constant D) when a 0.33 m impeller was used in the three tanks with a clearance of $T/3$, the circulation path increased, resulting in a positive exponent over T . In the second set (constant D/T ratio), when 0.10, 0.19, 0.33, and 0.5 m dia. impellers were used in 0.3, 0.57, 1.0, and 1.5 m tanks, although the clearance increased with increasing T , the diameter also increases. The overall effect of impeller diameter and tank diameter results in a negative exponent. The exponent over D in Eq. 3 was obtained while keeping T constant and varying D , whereas in Eq. 6 D was kept constant and T was varied. There-

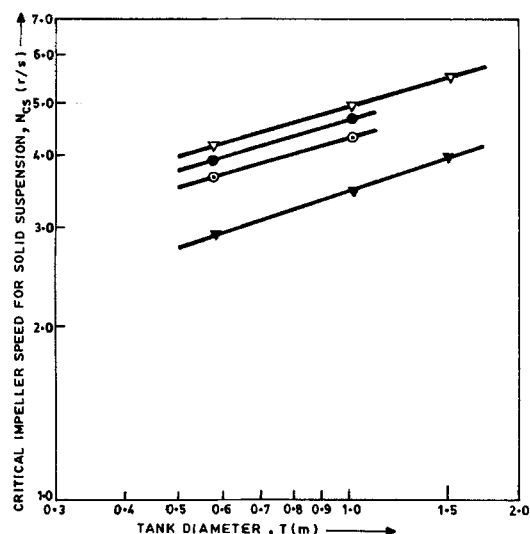


Figure 9. Effect of tank diameter at constant PTD impeller diameter on critical impeller speed for solids suspension.

$C = T/3$; $D = 0.33$ m
 X , wt. % d_p , μ m

○	6.6	100
●	12.7	100
▼	0.66	100
▽	0.66	2,000

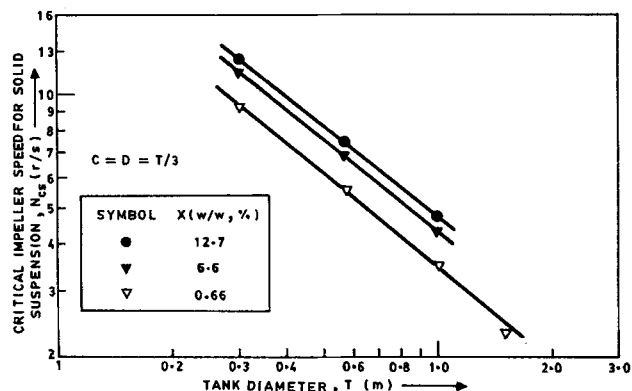


Figure 10. Effect of tank diameter on critical impeller speed for solids suspension at constant D/T ratio, PTD impeller.

$d_p = 100 \mu$ m

fore, when both D and T are varied simultaneously while scaling up, the exponent over D (or T) should be an overall effect of the above two situations. In other words, the exponent over D should be -0.85 . The obtained value of -0.82 in Eq. 7 is very close to this. The values of exponent over T reported by Zwietering (1958) and Chapman et al (1983) are -0.85 and -0.76 , respectively. These values are comparable to that obtained in the present work.

Correlation

When all the above observations are combined, the overall correlation for the critical impeller speed for solid suspension for a PTD impeller is given by:

$$N_{CS} = \frac{f\gamma^{0.1}(g\Delta\rho/\rho_L)^{0.45}X^{0.1}d_p^{0.11}T^{0.31}}{D^{1.16}} \quad (\text{std. dev.} = \pm 2.5\%) \quad (8)$$

where the average f value was found to be 3.3.

In the same expression, if the effect of the T/D ratio is taken in the constant s , it will take the following form:

$$N_{CS} = \frac{s\gamma^{0.1}(g\Delta\rho/\rho_L)^{0.45}X^{0.1}d_p^{0.11}}{D^{0.85}} \quad (9)$$

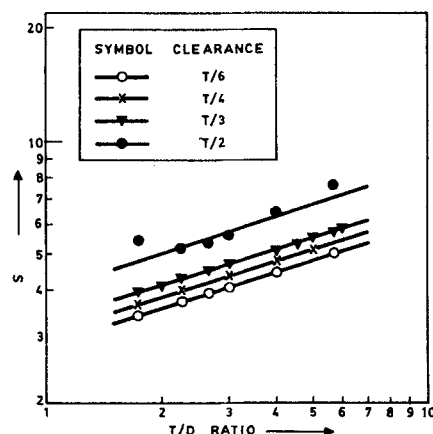


Figure 11. Proportionality constant s vs. T/D ratio, PTD impeller.

The values of s are plotted in Figure 11 against the T/D ratio for the entire range of variables, such as X , d_p , D , C , and T . The following relation was obtained using 250 data points:

$$s \propto (T/D)^{0.31} \quad (10)$$

Equations 8 and 9 are similar to that developed by Zwietering (1958), except the dependence on impeller diameter and tank diameter. Here, it is to be noted that Eq. 9 is exclusively for a PTD impeller whereas Zwietering's equation is for both a disk turbine and a propeller. It appears that the effects of impeller and tank diameters are different for different impeller designs.

Effect of blade width and blade thickness

In order to make the work more comprehensive, it was thought desirable to study the effect of blade width and blade thickness on critical impeller speed. To achieve this objective, 0.19 and 0.33 m dia. PTD impellers of different blade widths and thicknesses (details given in Table 2) were employed in 0.57, 1.0 m ID vessels. The solids loading was varied from 0 to 30 wt. % and the particle size was 100 μm .

The results are shown in Figures 12 and 13. To study the effect of blade width, W , its value was varied between 0.25 and 0.4 D , as shown in Table 2. It can be seen in Figure 12 that the value of N_{CS} initially decreases with an increase in blade. However, the extent of decrease reduces with further increase in blade width and a minimum value is observed at 0.35 D . Finally, when the width is increased from 0.35 to 0.4 D , the value of N_{CS} is found to increase.

The visual observations give a hint regarding such behavior. As the blade width increases both the axial and radial flow from the impeller increases. The increase in the axial component favors the suspension, whereas the increase in the radial component hampers the suspension because it counters the axial flow rising along the tank wall. Moreover, it appears that with an increase in blade width, the extent of increase in the radial flow is relatively more, compared with the extent of increase in the axial flow. Therefore, an increase in blade width does not proportionally decrease N_{CS} . In fact, the extent of reduction in N_{CS} decreases with an increase in W up to W/D of 0.35. Above this

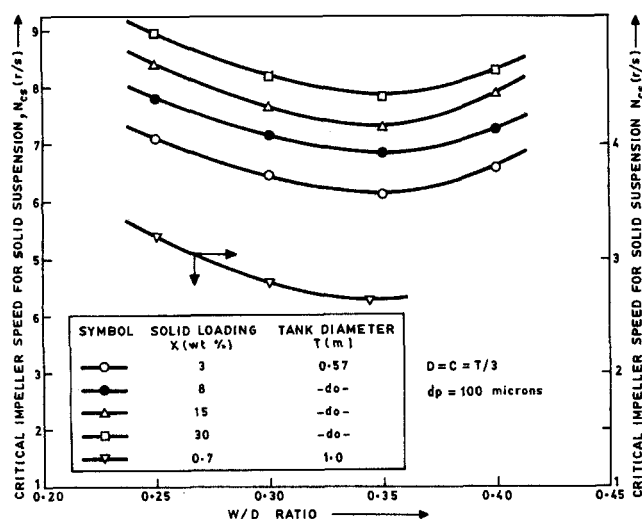


Figure 12. Effect of impeller blade width on critical impeller speed for solids suspension.

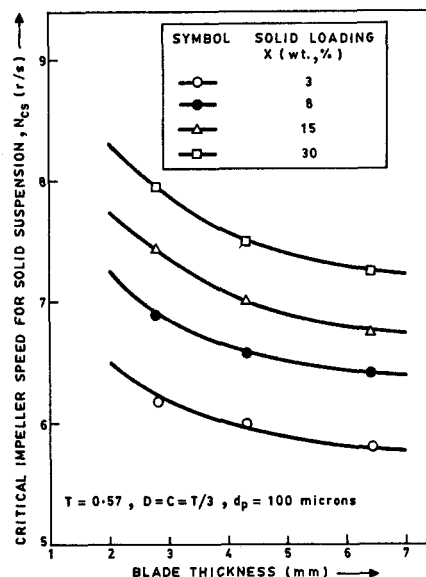


Figure 13. Effect of impeller blade thickness on critical impeller speed for solids suspension.

value, the radial component dominates the flow pattern and N_{CS} starts increasing with blade width. The contoured-blade airfoil type of pitched-blade impeller (A310 impeller, Gray and Oldshue, 1986) supports the above discussion. This modified design has a tapered inner edge of the blade so that there is a considerable decrease in the radial flow. As a result, at the same power consumption, the axial flow for the A310 impeller is greater, compared with a conventional PTD impeller.

In order to study the effect of blade thickness, a 0.35 D PTD impeller was selected and the thickness, k , was varied from 2.8 to 6.4 mm. The solids loading was varied from 0 to 30 wt. %. The results are shown in Figure 13 and can be correlated by the following expression:

$$N_{CS} \propto (k)^{-0.07} \quad (11)$$

The value of N_{CS} slightly decreases with an increase in blade thickness.

Increasing the blade thickness of an impeller (while keeping the other design parameters constant) increases the power consumption. As the type of flow pattern remains practically the same, the increased power may increase the average liquid flow and turbulence, thereby causing a slight decrease in the value of N_{CS} .

Conclusions

1. For the suspension of solid particles the pitched-blade turbine, downflow (PTD) was found to be most energy efficient.
2. The following correlation was obtained for the critical impeller speed for suspension of solid particles, N_{CS} , in the case of a PTD impeller:

$$N_{CS} = \frac{f \gamma^{0.1} \left(\frac{g \Delta \rho}{\rho_L} \right)^{0.45} X^{0.1} d_p^{0.11} T^{0.31}}{D^{1.16}}$$

for $100 < d_p < 2,000$ μm , $0 < x < 50$ wt. %, $0.175 < D/T < 0.58$, $W/D = 0.3$

The exponents over d_p and X were found to be practically the same as those of Zwietering (1958). However, the exponents on D and T were found to be different. The value of f depends upon impeller clearance.

3. In the case of disk turbine (DT) and pitched-turbine upflow (PTU) impeller, the exponents over d_p and X were essentially the same as those reported by Zwietering (1958).

4. The value of N_{CS} was found to decrease with a decrease in the impeller clearance from the bottom. The effect is substantial for DT and PTU impellers and relatively less pronounced for a PTD impeller. And the effect of clearance was found to be slightly diameter-dependent in the case of a PTD impeller.

Acknowledgment

This work was supported by a project sponsored under the Indo-US Materials Science Program.

Notation

- C = impeller clearance from tank bottom, m
- d_p = average particle size, μm
- D = impeller diameter, m
- f = constant, Eq. 8
- g = gravitational constant, m/s^2
- H = height of clear liquid above tank bottom, m
- k = blade thickness, m
- l = blade length, m
- L = path length of liquid flow, m
- N_{CS} = critical impeller speed for solid suspension, r/s
- N_{PSL} = power number in solid-liquid system
- s = proportionality constant, Eq. 1
- T = tank diameter, m
- V_r = radial velocity in the impeller stream, m/s
- W = blade width, m
- X = solid loading, wt. %

Greek letters

- γ = kinematic viscosity, m^2/s
- ρ_L = density of liquid, kg/m^3
- ρ_S = density of solid, kg/m^3
- $\Delta\rho = \rho_S - \rho_L$
- θ_{mix} = mixing time, s

Literature Cited

- Baldi, G., R. Conti, and E. Alaria, "Complete Suspension of Particles in Mechanically Agitated Vessels," *Chem. Eng. Sci.*, **33**, 21 (1978).
- Bohnet, M., and G. Niesmak, "Distribution of Solids in Stirred Suspensions," *Ger. Chem. Eng.*, **3**, 57 (1980).
- Bourne, J. R., and R. N. Sharma, "Homogeneous Particle Suspension in Propeller-Agitated Flat-Bottomed Tanks," *Chem. Eng. J.*, **8**, 243 (1974).
- Chapman, C. M., A. W. Nienow, M. Cooke, and J. C. Middleton, "Particle-Gas-Liquid Mixing in Stirred Vessels. 1: Particle-Liquid Mixing," *Chem. Eng. Res. Des.*, **61**, 71 (1983).
- Chudacek, M. W., Solid Suspension Behavior in Profiled-bottom and Flat-bottom Mixing Tanks," *Chem. Eng. Sci.*, **40**, 385 (1985).
- Einenkel, W., "Influence of Physical Properties and Equipment Design on the Homogeneity of Suspensions in Agitated Vessels," *Ger. Chem. Eng.*, **3**, 118 (1980).
- Gray, J. B., and J. Y. Oldshue, *Agitation of Particulate Solid-Liquid Mixtures*, Academy Press, **II**, 1-61 (1986).
- Harriott, P., "Mass Transfer to Particles. I: Suspended in Agitated Tanks," *AIChE J.*, **8**, 93 (1962).
- Joshi, J. B., A. B. Pandit, and M. M. Sharma, "Mechanically Agitated Gas-Liquid Reactors," *Chem. Eng. Sci.*, **37**, 813 (1982).
- Kneule, F., "Die Prufung von Ruhrem durch Loslichkeitsbestimmung," *Chem. Ing. Tech.*, **28**, 221 (1956).
- Kolar, V., "Studies on Mixing. X: Suspending Solid Particles in Liquids by Means of Mechanical Agitation," *Coll. Czech. Chem. Commun.*, **26**, 613 (1961).
- Musil, L., J. Vlk, and H. Jiroudkova, "Suspension of Solid Particles in Agitated Tanks with Axial-type Impellers," *Chem. Eng. Sci.*, **39**, 621 (1984).
- Narayanan, S., V. K. Bhatia, D. K. Guha, and M. N. Rao, "Suspension of Solids by Mechanical Agitation," *Chem. Eng. Sci.*, **24**, 223 (1969).
- Nienow, A. W., "Suspension of Solid Particles in Turbine Agitated Baffled Vessels," *Chem. Eng. Sci.*, **23**, 1453 (1968).
- Pandit, A. B., and J. B. Joshi, "Mixing in Mechanically Agitated Gas-Liquid Contactors, Bubble Columns, and Modified Bubble Columns," *Chem. Eng. Sci.*, **38**, 1189 (1983).
- Subbarao, D., and V. K. Taneja, "Three-phase Suspension Agitated Vessels," *Proc. 3rd Eur. Conf. Mixing*, **1**, 229 (1979).
- Weismann, J., and L. E. Efferding, "Suspension of Slurries by Mechanical Mixtures," *AIChE J.*, **6**, 419 (1960).
- Zwietering, Th. N., "Suspending of Solid Particles in Liquid by Agitators," *Chem. Eng. Sci.*, **8**, 244 (1958).

Manuscript received Oct. 5, 1987, and revision received Mar. 10, 1988.